Journal of Physics: Conference Series **500** (2014) 032016 doi:10.1088/1742-6596/500/3/032016

Measurement of the principal quasi-isentrope of lead to ~3Mbar using the "Z" machine.

S Rothman[1], J-P Davis[2], S Gooding[1], M Knudson[2] and T Ao[2]

[1]AWE Aldermaston, Reading, RG7 4PR, UK.
[2]Sandia National Laboratory, Albuquerque, NM, 87185, USA.

steve.rothman@awe.co.uk

Abstract. We have measured the principal quasi-isentrope of pure lead to ~3 Mbar, using magnetically-driven ramp compression on SNL's "Z" machine. Multiple point-VISARs were used to measure the surface velocities of the compressed samples, and iterative Lagrangian analysis was used to find the wave speed as a function of ramp velocity to an accuracy of <2%. This was then integrated to longitudinal stress as a function of volume on the quasi-isentrope. The experiment used a stripline configuration with samples arranged in pairs at each of 4 vertical positions on opposite drive panels: three of the four pair positions held two lead samples of different thicknesses, while the fourth consisted of one lead sample and a bare panel for drive measurement. The thicker samples of the 3 pairs experienced weak shocks at low stress so their quasi-isentrope data is unreliable there. The single-sample data was good at low stress but affected at high stress by either effects of closure of the stripline gap and / or reflections of the compression pulse from the drive-panel rear surfaces. Data from both methods overlapped at intermediate stresses so have been combined to give the required quasi-isentrope data.

1. Introduction

Quasi-isentropic compression experiments (ICE) are now a standard method of achieving high-pressure states and returning equation-of-state (EoS) and strength data [1-4].

We aimed to measure the principal isentrope of lead to ~3 Mbar, with 2% accuracy in sound speed, in order to assess the various EoS models available, in particular SESAME and an AWE multiphase model [5].

2. Method

Magnetic-pressure drive on Z was used to shocklessly compress a set of lead samples.

A vertical stripline of 2 parallel aluminium panels, shown in figure 1, labelled "North" and "South", had 4 pairs of opposing counterbores: each pair, or vertical location numbered 1 to 4, should experience the same drive despite any top-bottom magnetic-field variations. The top 3 locations held pairs of different-thickness lead samples, the bottom location had only one lead sample.

Lead discs were machined using a Precitech Nanoform diamond-turning lathe, and measured by a Nikon Nexiv CNC video measuring system, with laser profile scanning, and a Zygo white-light interferometer. The accuracy of the thickness measurements was mostly ±0.2 μm, indicating parallelism to this level. Density was found by displacement to be 11.33±0.05 gcm^{-3}. Thicknesses were chosen to give the maximum difference between pairs while ensuring no shocking and no return of the free-surface reflction to the Al/Pb interface; assuming a variety of different lead EoSs.

Content from this work may be used under the terms of the Creative Commons Attribution 3.0 licence. Any further distribution of this work must maintain attribution to the author(s) and the title of the work, journal citation and DOI.
Published under licence by IOP Publishing Ltd

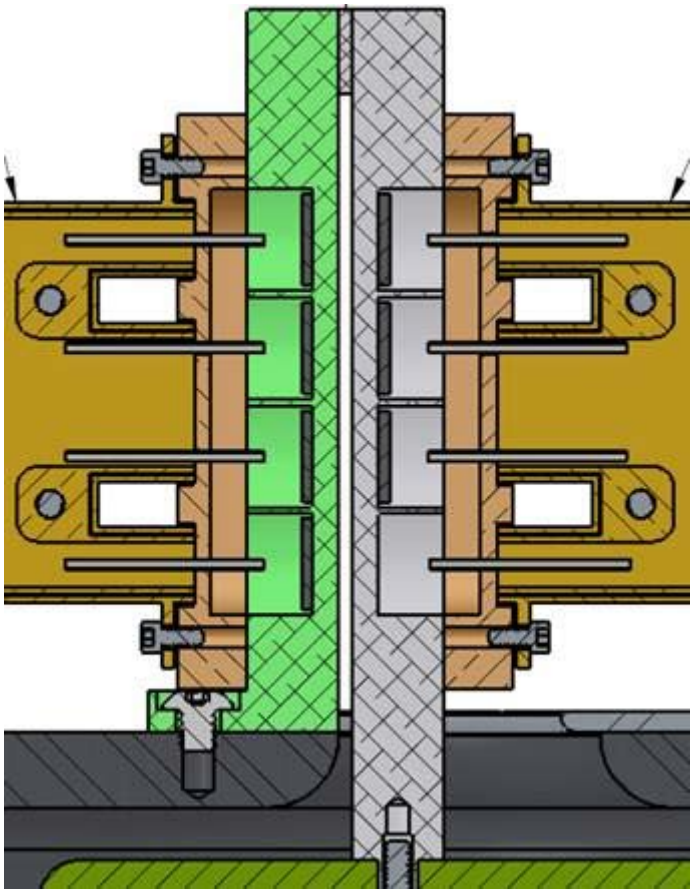

Figure 1. Schematic of stripline showing South (left) and North (right) panels with four vertical locations with opposing sample counterbores. VISAR probes monitor each sample or drive panel surface.

Each sample, and the bare Al drive panel, was monitored by 2 point VISARs with different velocity-per-fringe (VPF).

Shockless compression was produced by a slowly-rising current pulse which was calculated by iterative MHD code calculations to match the desired free-surface velocity profiles.

3. Results

All VISARs returned good data, as shown in figure 2.

The thicker lead samples shocked at low pressure – velocities <1.1 kms^{-1} and <1.7 kms^{-1} - but it is hoped that the Hugoniot here is close to the isentrope and the standard analysis will work but with the shocking manifesting as a small error. These velocities correspond to particle velocities of ~0.55 and 0.85 kms^{-1}, pressures of 0.2 and 0.32 Mbar. These are above the known phase change at 0.13 Mbar, so are probably due to local evolution of the ramped pulse into shocks.

The velocity for sample N1 (top of the North stripline), a 900 μm sample, becomes earlier and higher than the 775 μm samples at late time. Similarly, S4, the single 850 μm sample, becomes later and lower than the ~900 μm samples, indicating magnetic pressure decreasing from top to bottom. However, if the pressure is equal on the N and S panels at each vertical location the analysis should be unaffected.

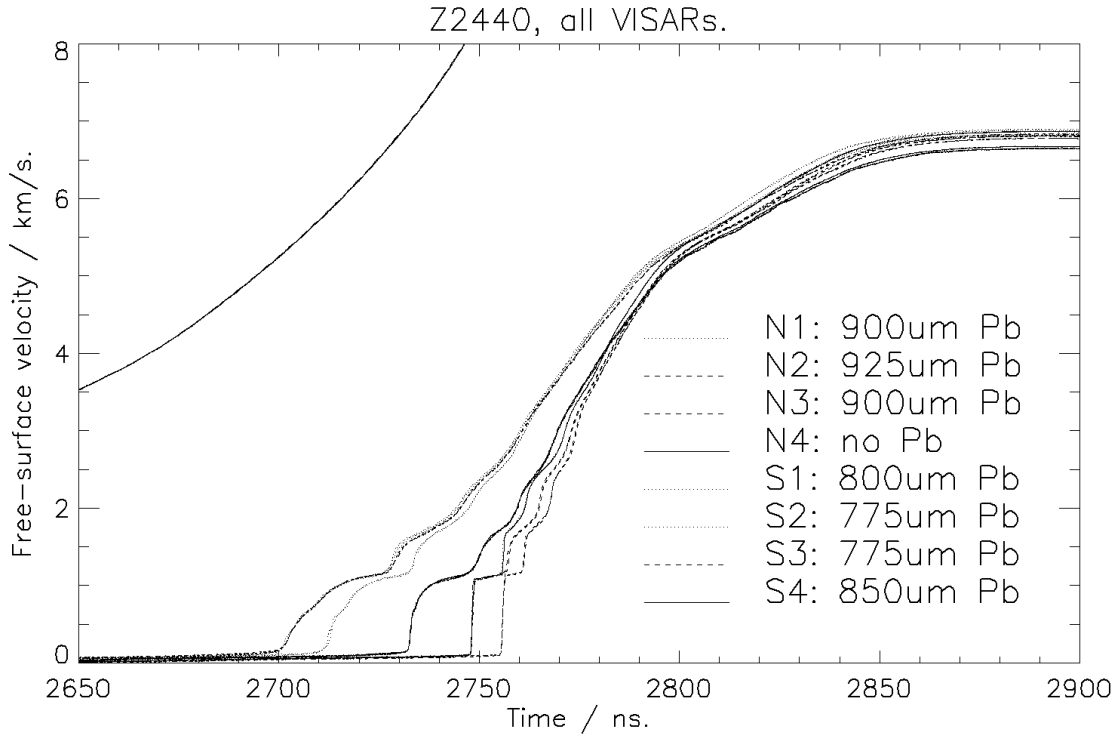

Figure 2. Free-surface velocity-time for all VISARs (2 per sample).

4. Analysis methods

Free-surface velocity needs to be converted to *in-situ* particle velocity, and then the arrival times of a velocity at different thicknesses of lead give Lagrangian sound speed at that particle velocity. Three characteristics-based methods were used to analyse the data.

4.1. Iterative Lagrangian analysis (ILA)

An initial assumed EoS (or the *in-situ* velocity equals half the free-surface velocity approximation) is used to convert free-surface velocity to *in-situ* velocity for two different-thickness lead samples, and Lagrangian sound speed as a function of particle velocity, $c_L(u_p)$, found from the thickness difference divided by the difference in arrival times of the velocity. This is integrated to longitudinal stress, $d\sigma = \rho_0.c_L(u_p).du_p$ and specific volume, $dV = -du_p / \rho_0.c_L(u_p)$. From this new $\sigma(V)$ the velocity correction can be iterated until the sound speed converges. This is described in [6].

4.2. Hinch method

Free-surface velocities of two samples are interpolated onto a regular grid, which makes sound speed take on a discrete set of values corresponding to these velocities, and to the intersections of the two grids of incoming and reflected characteristics [7-8]. Using the ambient sound speed the next higher sound speed is found, and successively higher sound speeds found in turn. This is a single-pass method, and no interpolation of EoSs is needed.

This method was compared with the ILA method and both were in agreement. The raw VISAR data was sampled at 25 ps intervals and this was resampled for faster analysis. The ILA tended to become noisy with a small number of points, while the Hinch analysis became unstable with larger numbers of points. A convergence test indicated that ILA was good with 1000 points and this was used for most analyses.

4.3. Single-sample or "zero-thickness" method

This is based on the method developed by J-P Davis [9-10]. A measurement of a bare drive-panel free-surface velocity is converted to *in-situ* with an assumed Al EoS, and a forward characteristics calculation of the velocity there would be in a notional lead sample is made. This is then used with the opposed lead sample velocity measurement to do an ILA. The advantages are that an intermediate-thickness sample may be used, which is less liable to both shocking and reflection effects, and the thickness difference here is the sample thickness, ~850 μm. The fractional errors are then reduced by a factor of ~7 compared with the pairs with thickness differences of 100-150 μm. The main disadvantage is that it is limited by the return of the reflections from the driver free surface, and driver/sample interface, after which the bare drive panel and sample see different drives. The characteristics calculations may account for this to some extent, but when differential motion of the drive surfaces affect the MHD physics the analysis will fail.

5. Sound-speed and stress-volume data

As two VISARs monitored each sample then each pair location gives 4 datasets for sound speed. These were found to fall into two pairs of similar results, which may be attributed to VISAR synchronisation. A Gaussian timing fiducial is introduced into the laser pulse, but this is split in two by the interferometer and then recombined as a pair of Gaussians separated by the étalon delay (~1 or 0.6 ns here); the timing software looks only to fit a single Gaussian peak. To assess timing effects the VISAR data was interpolated onto a velocity grid and time differences between VISARs on the same sample found. These were generally "good" (<50 ps) or "poor" (0.1<dt<0.4 ns). For each stripline location, one pair of sound speeds generally corresponded to a well-synchronised VISAR pair and one of the poorly-synchronised VISARs on the other sample, while the other pair was the well-synchronised pair and the other poorly-synchronised VISAR. The magnitude and sense of the time differences agreed with the differences in sound speed.

Figure 3 shows the sound-speed data for all pairs, and the single-sample analysis. There is a clear trend of increasing sound speed from position 1 to 3 (top to bottom of the stripline) which does not seem to correlate with lead thicknesses or thickness differences. While there is decreasing drive top to bottom, this should not affect sound-speed results unless the drive is different on the two panels.

The velocity-data arrival times were corrected for drive-panel thickness-differences, but not for glue-bond thickness and possible compression of the lead samples on assembly to the panels. The combined glue and sample thicknesses were measured but had large scatter, including some apparent negative bond thicknesses. Glue bond thicknesses were expected to be sub-micron.

The single-sample results are good at low particle velocity, in particular they do not have the oscillations arising from the shocks that the paired analyses have. However the sound speed is clearly wrong at high particle velocity after the drive-panel free-surface reflection returns to the drive surface. It is hoped that the analysis can be modified to account for this: preliminary results show that characteristics can correctly calculate reflections.

While figure 3 shows that the scatter or systematic error in sound speed is of order ±0.1/1.5 or ±~6%, the estimated errors from sample thickness, VISAR synchronisation, and VISAR velocity errors (Δu=0.02.VPF) converted to time errors, are ~2%. (Propagation of errors in the Hinch analysis method gives results less than simplistic ones based on the sample thickness difference, and transit time from this and sound speed). For position 2 with the worst synchronisation error of 0.4 ns this error dominates, the thickness errors are negligible, and the velocity error is only significant just after the peaks of the low-pressure shocks and at late time when du/dt is small and $\Delta t = \Delta u / (du/dt)$ is large.

We had fired two earlier shots - Z753 and Z770 – on lead to lower pressure [11]. The mean sound speed of bulk lead from these shots is compared with the low-pressure position 4 result in figure 4a.

Agreement with the prior results is excellent within their errors.

Figure 4b shows a comparison between representative position 2 stress-volume data and the SESAME 3200 [12] and AWE multiphase [5] principal isentrope P(V) data: the data agree with SESAME within the experimental errors; only partially with the AWE model.

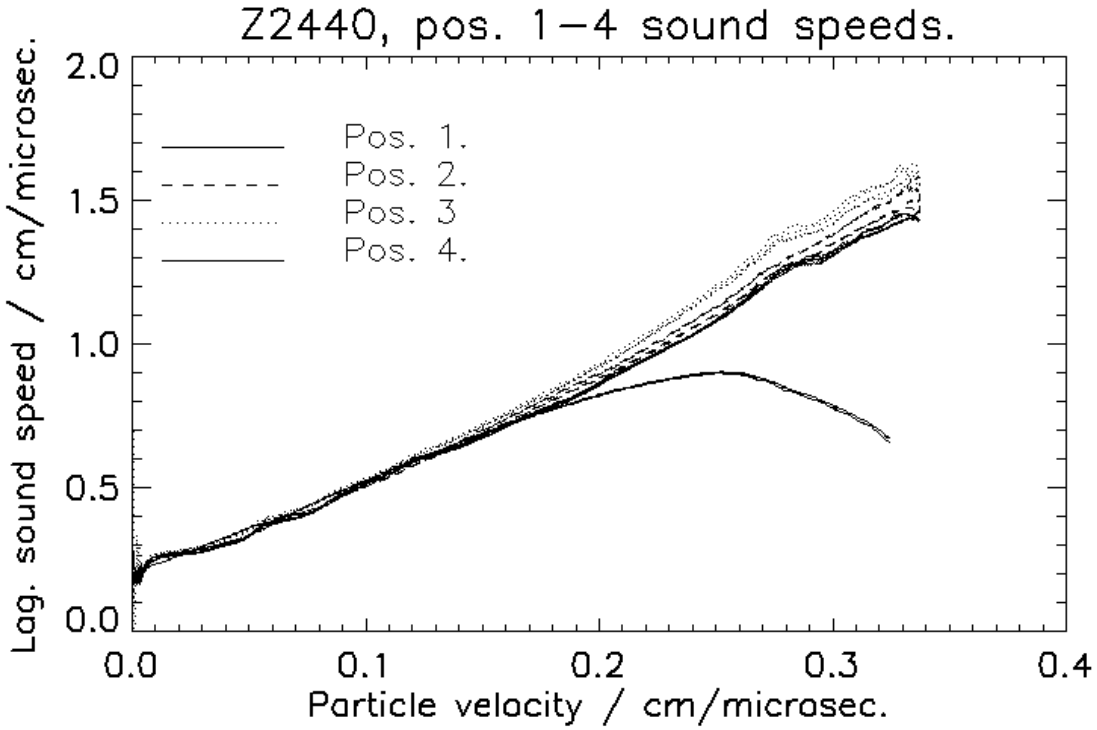

Figure 3. Sound speed vs particle velocity from all 4 locations.

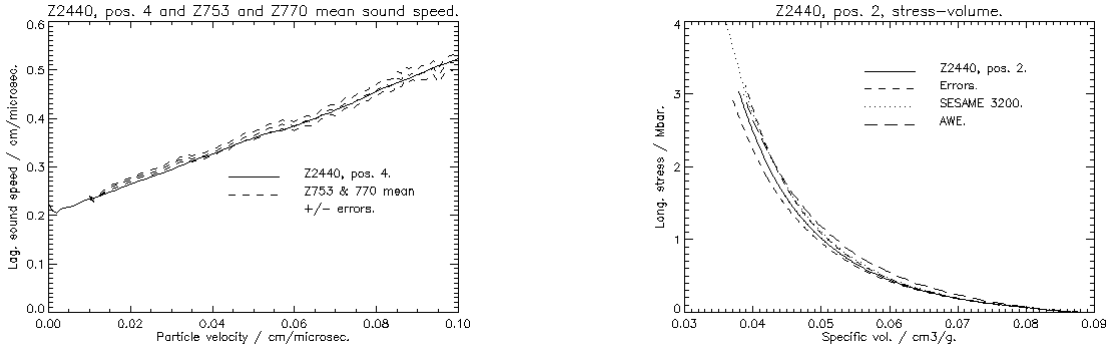

Figure 4. a) Comparison of sound speeds from lower-pressure shots Z753 and Z770 with position 4 data from current shot. b) Stress-volume from representative mean position 2 data compared with SESAME EoS and AWE P(V) models for lead.

6. Summary and conclusions

We have shocklessly compressed lead to ~3 Mbar (though low-pressure shocks in some samples affect some analyses). Multiple measurements of sound speed as a function of particle velocity have been

made from multiple VISAR measurements, and by different methods. All three analysis methods are consistent apart from the failure at high-pressures of the single-sample analysis, which we think may be corrected, or analysed using a hydrocode-based analysis [9-10].

The main issue is an apparent systematic trend in sound speed from top to bottom of the stripline, which does not correlate with lead sample thicknesses. A top-bottom drive variation is evident but should not give a similar trend in sound speeds.

VISAR synchronisation has been identified as one significant source of error but may be eliminated by a reanalysis of the timing data – and the timing method on future Z shots can be changed to correct this. Glue-bond thickness and possible lead-sample compression remain as unquantified errors.

If the variation in sound speed is random, then a mean (of 3 means of four pair results for each position) sound speed should have scatter reduced by a factor slightly greater than $\sqrt{3}$ to ±~3%, while propagated errors are ~2%.

Conversion of sound speed to stress-strain (volume) awaits resolution of any systematic error, but a preliminary comparison of representative position 2 pair data is in reasonable agreement with SESAME and AWE EoS models for lead.

References

[1] Davis J-P 2006 *J. Appl. Phys.* **99** 103512
[2] Bradley D K, Eggert J H, Smith R F, Prisbrey S T, Hicks D G, Braun D G, Biener J, Hamza A V, Rudd R E and Collins G W 2009 *Phys. Rev. Lett.* **102** 075503
[3] Ao T, Knudson M D, Asay J R and Davis J-P 2009 *J. Appl. Phys.* **106** 103507
[4] Nguyen J H, Orlikowski D, Streitz F H, Moriarty J A and Holmes N C 2004 *AIP Conf. Proc.* **706** 1225-8
[5] Mehta S 2007 Theoretical melt curves of Al, Cu, Ta and Pb *AIP Conf. Proc.* **955** 258-61
[6] Rothman S D and Maw J R 2006 *J. Phys.* IV **134** 745-50
[7] Hinch E J 2010 *J. Eng. Math.* **68**(3-4) 279-89
[8] Ockendon H, Ockendon J R and Platt J 2010 *J. Eng. Math.* **68**(3-4) 269-77
[9] Davis J-P and Knudson M D 2009 *AIP Conf. Proc.* **1195** 673-6
[10] Davis J-P 2013 Analysis of data from shockless compression experiments to multi-megabar pressure *submitted to these proceedings*
[11] Rothman S D, Davis J-P, Maw J R, Robinson C M, Parker K and Palmer J 2005 *J. Phys.* D.: *Appl. Phys.* **38** 733-40
[12] Barnes J and Rood J SESAME 3200 *Los Alamos National Laboratory Tech. Rep.* LA-10160-MS2